Energy and Buildings 127 (2016) 907–919

Contents lists available at ScienceDirect

Energy and Buildings

journal homepage: www.elsevier.com/locate/enbuild

Optimized performance of displacement ventilation aided with chair fans for comfort and indoor air quality

Walid Abou Hweij, Nesreen Ghaddar*, Kamel Ghali, Carine Habchi

Mechanical Engineering Department, Faculty of Engineering and Architecture, American University of Beirut, P. O. Box 11-0236, Beirut, 1107-2020, Lebanon

ARTICLE INFO

Article history:
Received 22 April 2016
Received in revised form 14 June 2016
Accepted 16 June 2016
Available online 16 June 2016

Keywords:
Displacement ventilation
Chair fans
Thermal comfort
Indoor air quality
Energy savings

ABSTRACT

This study optimizes the performance of displacement ventilation (DV) system aided with chair fans (CF) for providing acceptable thermal comfort and indoor air quality (IAQ) in office space. A 3-D computational fluid dynamics (CFD) model coupled with a bio-heat model was used to predict the airflow, temperature, and CO_2 concentrations fields as well as the occupant segmental skin temperatures for local and overall thermal sensation and comfort evaluation. The CFD model results were validated experimentally in a DV conditioned space using a thermal manikin seated on a chair equipped with fans.

Simulations were performed using the validated CFD model to determine the fans optimal height from the floor. For a pollution source located at 1.0 m from the floor, it is recommended to place the fans at 30.9 cm above the floor at fans total flow rate of 12 L/s while for a pollution source located at 0.3 m from the floor, the optimal height of fans is at 30.1 cm above the floor at fans total flow rate of 12 L/s. Compared to stand alone DV system, energy savings were 20.6% and 11.6% for fans' optimal heights of the sources placed at 1.0 m and 0.3 m, respectively.

© 2016 Elsevier B.V. All rights reserved.

1. Introduction

Acceptable thermal comfort and good indoor air quality (IAQ) are the main requirements to be provided by ventilation systems in open space office buildings. Displacement ventilation (DV) system supplies 100% fresh and cool air at low velocity near the floor level from a wall mounted diffuser relying on heat sources that push the resulting warm and polluted air by buoyancy to the upper room level to be exhausted; thus creating temperature stratification within the space [1]. This system requires the conditioning of the 100% fresh air supply stream which is energy intensive compared to mixed streams used in conventional. Additionally, the restrictions on the supply air temperature (not to be less than 18 °C) and flow velocities (not to be more than 0.2 m/s) [2,3], hindered the DV system from removing high internal loads. Thus, DV system might not be cost effective in hot and humid climate conditions. Furthermore, Brohus et al. [3,4] reported poor performance when a passive contaminated source existed at low level.

Several studies proposed different approaches to improve the performance of DV system. One approach was to use chair-mounted fans of an office occupant firstly proposed by Sun et al. [5–10]. Sun et al. [5,7] proposed the use of four computer fans placed at the corners of the chair. They surveyed participants about their thermal comfort while changing speed of the fans for different room air temperatures. Their study suggested the appropriate speed of fans that provided thermal comfort for occupants for the various room temperatures. Moreover, Sun et al. [7,8] investigated experimentally the effect of chair fans (CF) on an ambient passive contaminant represented by CO_2 tracer gas. The study showed that for the proposed configuration of fans (at the level of thighs), the fans increased the concentration of CO_2 at the occupant's breathing zone. Additionally, they found that the use of this novel system resulted in a reduction in energy consumption up to 19% [7]. Habchi et al. [11] studied the performance of DV system assisted by chair fans (DV + CF) in reducing particles transmission. They reported that the use of fans caused a reduction in inhalation effectiveness when compared to a standalone DV system. In addition, they reported that the novel system provided thermal comfort when assessed using predicted mean vote (PMV) model. Evidently, using CF in aiding DV system had noticeable effects on thermal comfort and particles transmission while reducing energy consumption.

All the previous studies focused on the use of CF at a fixed level without consideration of the effect of the height while varying fan flow rate on thermal comfort and IAQ. Recent study done by El-Fil et al. [12] showed noticeable improvements in thermal comfort and IAQ as a result of variations in height and flow rate of CF while

* Corresponding author.
E-mail address: farah@aub.edu.lb (N. Ghaddar).

http://dx.doi.org/10.1016/j.enbuild.2016.06.052
0378-7788/© 2016 Elsevier B.V. All rights reserved.

Nomenclature

Symbols

C_B	CO_2 concentration of the breathing zone (ppm)
C_{Fr}	CO_2 concentration of the fresh air (ppm)
C_r	CO_2 concentration of the recirculated air (ppm)
CF	Chair fans
CFD	Computational fluid dynamics
CPV	Ceiling personalized ventilation
DV	Displacement ventilation
DV + CF	Displacement ventilation assisted by chair fans
H_{fs}	Height of fans relative to floor (cm)
H_s	Height of source relative to floor (cm)
IAQ	Indoor air quality
LTC	Local thermal comfort
LTS	Local thermal sensation
MV	Mixed ventilation
PMV	Predicted mean vote
PPM	Parts per million
$\dot{Q}$	Total flow rate of fans (L/s)
RH	Relative humidity (%)
TC	Overall thermal comfort
TS	Overall thermal sensation
y	First inflation layer thickness (mm)
y^+	Dimensionless wall thickness (−)

Greek symbols

ε_v	Ventilation effectiveness (%)
ρ	Air density (kg/m^3)
μ	Air dynamic viscosity (Pa s)
τ_w	Wall shear stress (Pa)

aiding ceiling personalized ventilation system (CPV). In DV system, varying the height of the fans above the floor while varying their flow rate may affect the thermal comfort. Moreover, the use of CF at different heights and flow rates may affect the breathing air quality when passive contaminants are placed at different heights above the floor. To our knowledge, the effect of fans height above the floor and their flow rate on breathing air quality and comfort at different passive contaminant height above the floor has not been investigated in the literature.

Hence, this study will investigate the performance of (DV + CF) system with the purpose of optimizing the height of fans above the floor for different passive contaminant height. A computational fluid dynamics (CFD) model of the DV-conditioned space with chair fans is developed. The CFD model will be validated experimentally using thermal manikin to compare the segmental surface temperature and CO_2 contaminant concentration in the breathing zone at a specified source height. A parametric study will follow to assess the system performance in providing acceptable thermal comfort and good IAQ for an office occupant at low energy consumption.

2. Methodology

Fig. 1(a) shows a schematic diagram of (DV + CF) system. The supply diffuser supplies fresh air into the room, the thermal manikin represents an office occupant, the chair mounted fans, placed on each side, blow air upwards, the CO_2 tracer gas represents passive contaminants in the room, and the exhaust diffuser extracts contaminated air from the space. Fig. 1(b) and (c) shows in details the configuration of chair mounted-fans. The fans can move vertically up and down resulting in a controlled height $\left(H_{fs}\right)$ while supplying total flow rate $\left(\dot{Q}\right)$ equally distributed over the four fans.

To study the effect of various parameters; including height of fans above the floor, flow rate of fans, and passive contaminant source height above the floor, on the performance of (DV + CF), a 3-D CFD model is used to investigate the ability of the (DV + CF) system with the controllable height in providing comfortable environment while aiding the thermal plumes in delivering a relatively clean air at the breathing level of the occupants. Experiments are conducted to validate the findings predicted by the computational model. The predicted CO_2 concentration fields along with the segmental surface temperatures of the modeled occupant are then compared with the experimental measurements. Following the experimental validation, the CFD model is used to run a parametric study on a typical office space with specified load to assess and optimize the performance of the proposed system (DV + CF) under the effect of various parameters while providing low energy consumption.

2.1. CFD model

The complex interactions resulting from the upward jets of fans and the rising thermal plumes should be accurately predicted to assess their behavior on the thermal and CO_2 concentration fields. Similar studies done by Makhoul et al. [13] resulted in accurate prediction of the airflow and thermal patterns along with the CO_2 concentration fields. Thus, CFD modeling would be used to investigate the effectiveness of the proposed (DV + CF) system under different configurations.

2.1.1. Airflow modeling

The commercial software ANSYS© Fluent was selected for assessing the flow fields of indoor environment as shown in Fig. 2. Accurate prediction of the airflow, thermal, and CO_2 concentration fields are based on proper modeling of flow physics including turbulence models, buoyancy effects, and boundary layers near the surfaces [14]. Proper controlling of the grid resolution at some surfaces is crucial to capture perfectly the shear-layer entrainment process and the different thermal plumes as well as the fluid/thermal boundary layers around the occupant [13]. The flow behavior at the boundary layer is accurately predicted using inflation layers. The selection of the inflation layers is based on first layer thickness y such that the dimensionless number y^+ ranges between 0.8 and 4, in order to an accurately resolve the viscous sub-layer as reported in ANSYS online manual [15]. Accordingly, the first layer thickness based on a selected y^+ value is estimated as follows:

$$y = \frac{y^+ \mu}{\rho \mu_\tau} \tag{1a}$$

where ρ and μ are the air density and dynamic viscosity and μ_τ the friction velocity is given by:

$$\mu_\tau = \sqrt{\frac{\tau_w}{\rho}} \tag{1b}$$

where τ_w is the wall shear stress.

The boundary faces were set to different element sizes using tetrahedral unstructured grid. A grid independence test was performed. The mesh is considered independent when the maximum relative error between two consecutive grid sizes is less than 5%. Initially, a face size of 2 cm and 8 cm were assigned to the surfaces of the manikin and the walls respectively resulting in 766,144 elements and 184,707 grid nodes. The face size was increased where the temperature, velocity and concentration fields at certain locations were compared with the previous grid test. This was repeated until grid independence was assured. A total number of 3,516,946 elements and 876,576 grid nodes were selected to accurately predict the flow behavior with less computational cost as illustrated in Table 1. Fig. 3 represents (a) the generated grid for the computational domain and (b) generated grid for the manikin.

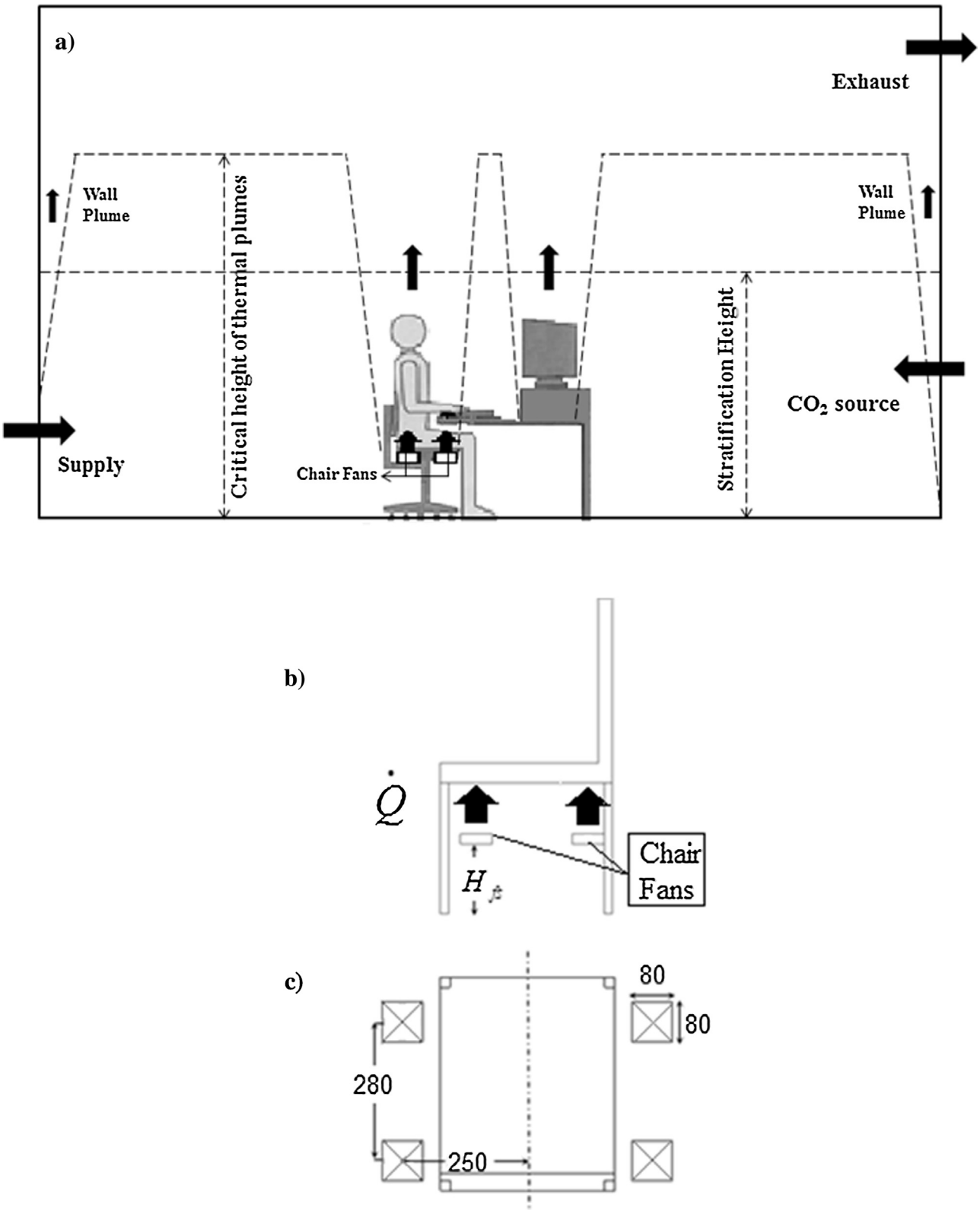

Fig. 1. (a) Schematic diagram of the proposed (DV + CF) system and chair mounted fans (b) chair side view and (c) chair top view. All dimensions on the drawing in millimeter.

Numerical modeling established by the commercial software ANSYS Fluent© is used to solve for the velocity, thermal, and species concentration fields within the space. The standard $k-\varepsilon$ turbulence model is selected based on its ability to predict accurate results that were validated experimentally in published literature [16–18]. The enhanced wall treatment option is selected to accurately predict the flow fields that involved separation and recirculation [13,15]. The Boussinesq approximation is used in the density modeling to account for buoyancy effects [15,18]. On the other hand, the species transport equation is used to assess the CO_2 concentration field [15]. The momentum, k, ε, energy and even the species transport differential equations are discretized using

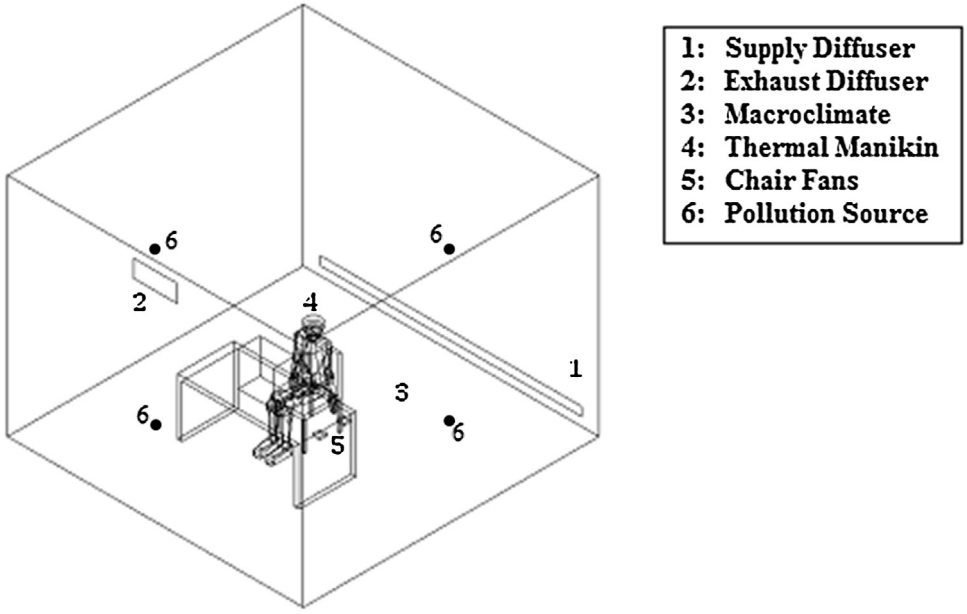

Fig. 2. The computational domain used in ANSYS (1) supply diffuser, (2) exhaust, (3) macroclimate, (4) thermal manikin, and (5) chair fans.

Table 1
Grid independence testing using five mesh cases.

Grid Type	Face Sizing (cm) Manikin/Walls	Number of Elements	Number of Grid Nodes	Maximum relative difference in predicted values of temperature velocity and concentration with the previous mesh values %
Mesh 1	2/8	766,144	184,707	–
Mesh 2	2/5	1,217,543	301,264	43.52
Mesh 3	1.5/3	2,559,155	638,040	10.32
Mesh 4	1.5/2.5	3,516,946	876,576	5.5
Mesh 5	1.5/2	5,652,622	1,384,638	4.4

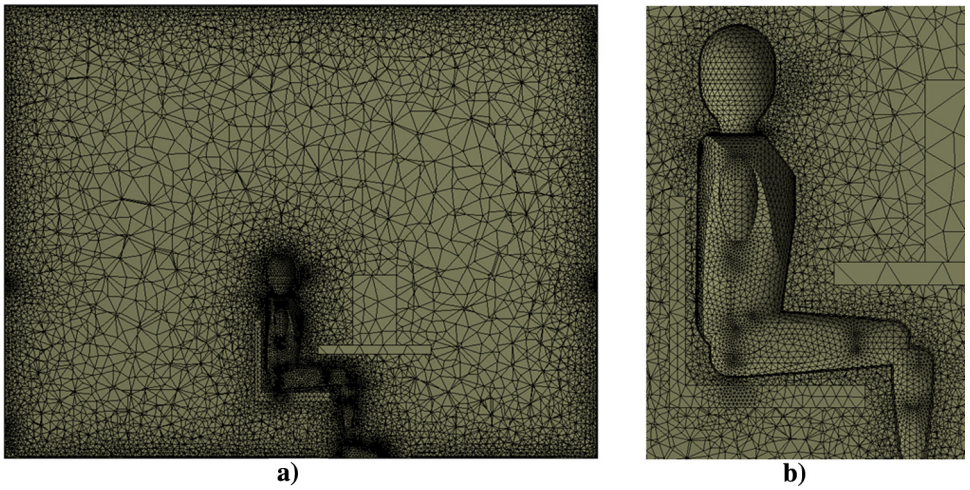

Fig. 3. (a) Mesh generation of the computational domain. (b) Mesh generation of the manikin.

the second order upwind scheme [15]. The "Standard" staggered scheme is used for the pressure [18] where the latter is coupled with velocity fields using the simple algorithm [15]. The numerical convergence criteria was based on assigning scaled residual of minimum value of 10^{-5}, monitoring the actual values at certain points, and having a net heat flux of the computational domain below 1% of the total heat gain [13].

2.1.2. Air quality modeling

The mixing between the supplied fresh air and the passive contaminants affect the level of air quality inside the room. Different studies in the literature used the CO_2 tracer gas as an indication of IAQ. In this work, this was done by measuring the concentration of CO_2 at the breathing zone of occupant relative to that at the exhaust

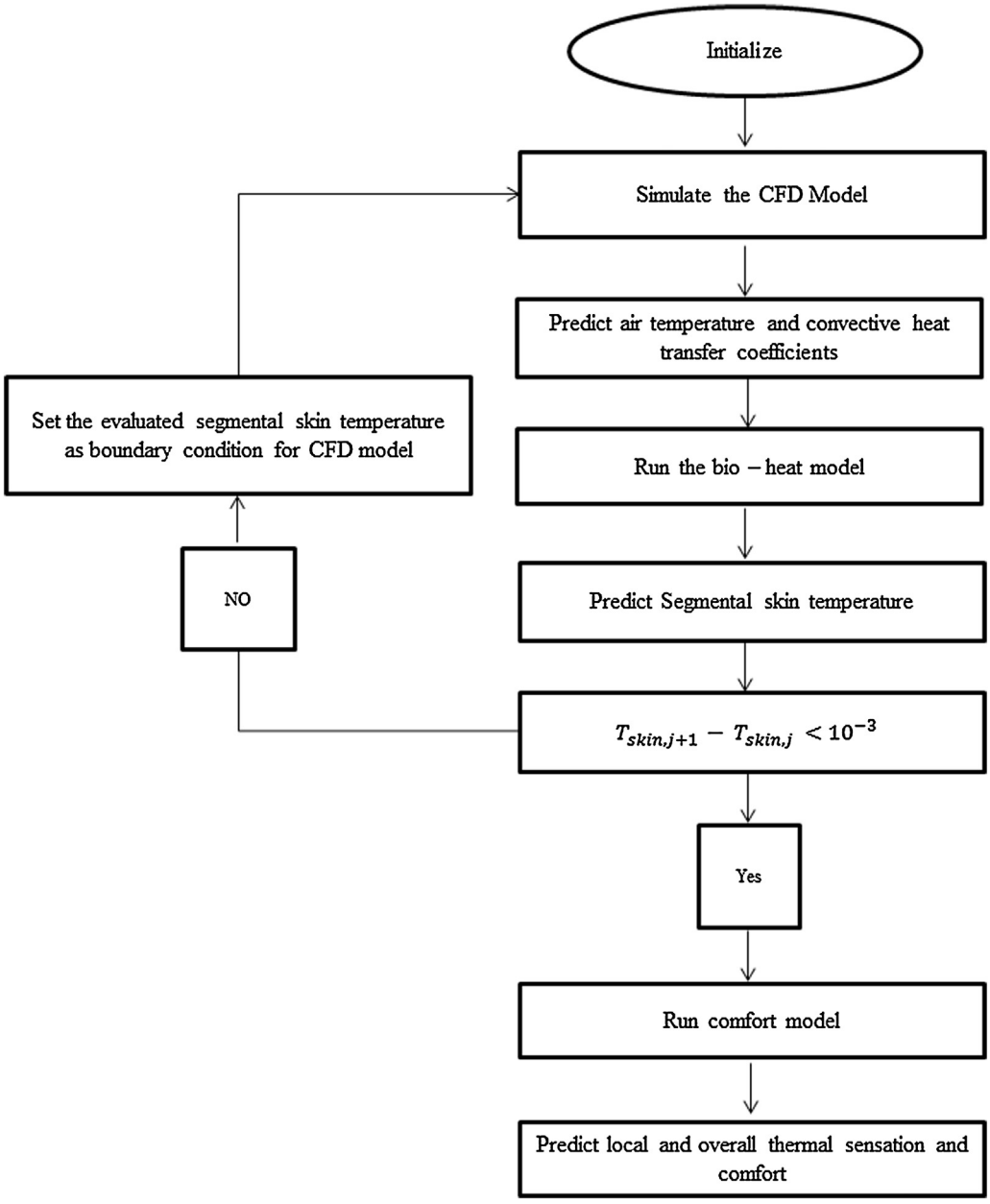

Fig. 4. Flow chart for the coupling of the CFD model with the bio-heat and comfort model.

and supply diffusers [13]. Hence, the ventilation effectiveness ε_v as expressed as follows:

$$\varepsilon_v = \frac{C_R - C_B}{C_R - C_{Fr}} \quad (2)$$

where C_R is the CO_2 concentration of the recirculated air, C_B is the CO_2 concentration at the breathing zone, and C_{Fr} is the CO_2 concentration at the supplied fresh air. Therefore, the higher the ventilation effectiveness the better will be the air quality.

Passive contaminant source represented by CO_2 tracer gas was placed at a certain height above the floor where it supplied CO_2 at a specified flow rate at room temperature. The polluting source was supplied through four identical sources such that each source was located on a wall to insure uniform distribution of CO_2 inside the room. Real fresh air in the range of 300–500 ppm is introduced via DV supply diffuser as recommended by ANSI/ASHRAE standard 62.1-2013 [19]. The concentration of inhaled air is measured as a volume average concentration in the spherical volume of 2 cm diameter placed at 2.5 cm from the manikin's nose [13].

2.1.3. Boundary conditions

Proper CFD modeling is based on the setting of boundary conditions to accurately predict airflow, thermal and CO_2 concentration fields. The supply diffuser and CO_2 source are set to a specified velocity inlet, temperature, turbulence intensity, CO_2 concentration, and hydraulic diameter. The exhaust diffuser is set to pressure outlet with zero gauge pressure at a specified turbulence intensity and hydraulic diameter. Fans inlets are set to "fan" boundary condition with a predefined pressure drop depending on fan's flow rate and fans outlets are set to "interior" boundary condition [13]. Finally, the walls and ceiling are set to constant heat flux.

2.1.4. Bio-heat coupling

In order to assess the effect of fans on the thermal performance of (DV + CF) system, a validated bio-heat model proposed by Sal-

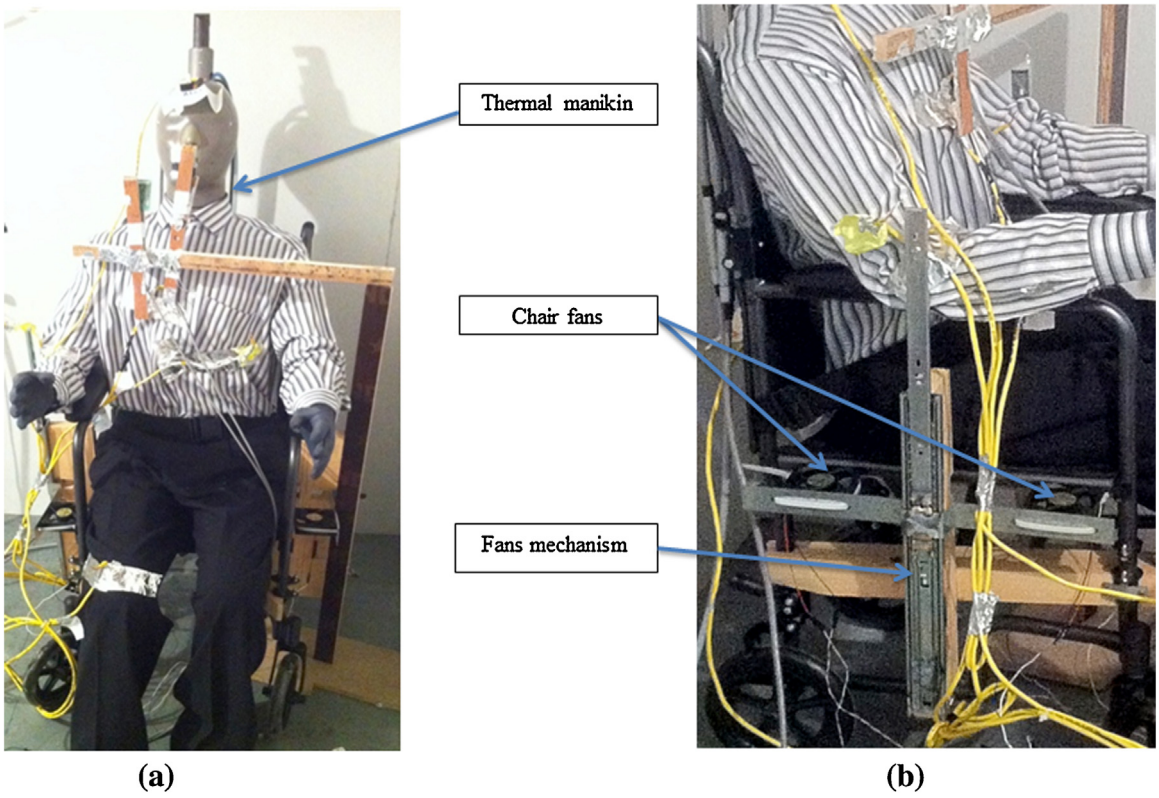

Fig. 5. Photos (a) thermal manikin used in the experiment (b) chair fan mechanism.

loum et al. [20] was coupled with the developed CFD model to accurately predict the occupant physiological response to the thermal environment. The prediction of occupant thermal comfort was evaluated using the models proposed by Zhang et al. [21–23]. The thermal comfort ranged from −4 (very uncomfortable) to +4 (very comfortable) where 0 referred to just comfortable. The thermal sensation scaled from −4 (very cold) to +4 (very hot) where −3 referred to cold, −2 to cool, −1, to slightly cool, +1 to slightly warm, +2 to warm, and +3 to hot [20–22]. The coupling between the CFD and bio-heat models is shown in Fig. 4.

Initially, in the CFD model, the manikin was set to conventional skin temperatures along with the proper settings for the energy, turbulence models, CO2 transport equations, and boundary conditions for different system components. Appropriate solution controls along with proper discretization schemes were assigned for the modeling equations. The bio-heat model divides the body into 11 segments (head, chest, back, abdomen, buttocks, U-arm, L-arm, hands, thighs, calves and feet). The prediction of physiological thermal responses of each body segment was based on the air temperature and the convective heat transfer coefficients at the vicinity of each body segment. The latter components were well predicted by the CFD model. The resulting segmental skin temperatures predicted by the bio-heat model were introduced as boundary condition for the occupant in the CFD model, where the coupling procedure would be repeated such that the difference between two consecutive iterations is less than 10^{-3}. Upon convergence, the predicted segmental skin temperatures were integrated with Zhang models to predict the local and overall thermal sensation and comfort.

2.2. Experimental setup

In this study, an experimental validation is crucial to reveal the ability of the CFD model in predicting the performance of (DV + CF) system. The configuration of (DV + CF) system used for the simulated room and the experimental set-up was held similar including all dimensions and input conditions. Additionally, the experimental thermal manikin standard dimensions provided by the manufacturer were used in the CFD simulation of the thermal manikin. Hence, the validation would be based on detailed comparison between the predicted and experimental data in the name of segmental surface temperature of occupant and ventilation effectiveness. Accordingly, three different sets of experiments were conducted. The fans were placed at two different levels while supplying constant flow rates, where their performance was compared to a standalone DV system. The DV supply diffuser was set to constant flow rate and temperature. The CO_2 source was located at a certain height above the floor similar to its location in the CFD modeling.

The experimental set-up consisted of a controlled climatic chamber ventilated by a DV system. The chamber was of inner dimensions of 2.5 × 2.75 × 2.8 m with supply and return grills cross-sectional area of 0.582 m (width) × 0.24 m (height) and 0.44 m (width) × 0.19 m (height) respectively. In this chamber, the thermal manikin "Newton" (see Fig. 5) manufactured by the Northwestern measured technology [24]. This manikin is characterized by high performance of ±0.1 °C temperature measurement and set-point control with a maximum heat flux of 700 W/m^2. "Newton" is subdivided into twenty different control zones where each zone can report the segmental surface temperature based on assigned constant heat flux. "Newton" is controlled through "ThermDAC" control software that is user-friendly Windows-based application providing all possibilities of control On the manikin's chair, four fans were placed, two at each side, having a single degree of freedom allowing them to move vertically up and down leading to a height ranging between 20 and 50 cm above the floor as shown in Fig. 5b. The dimensions of the fans were 80 mm (length) × 80 mm (Width) × 25.4 mm (height). These fans have a maximum DC volt-

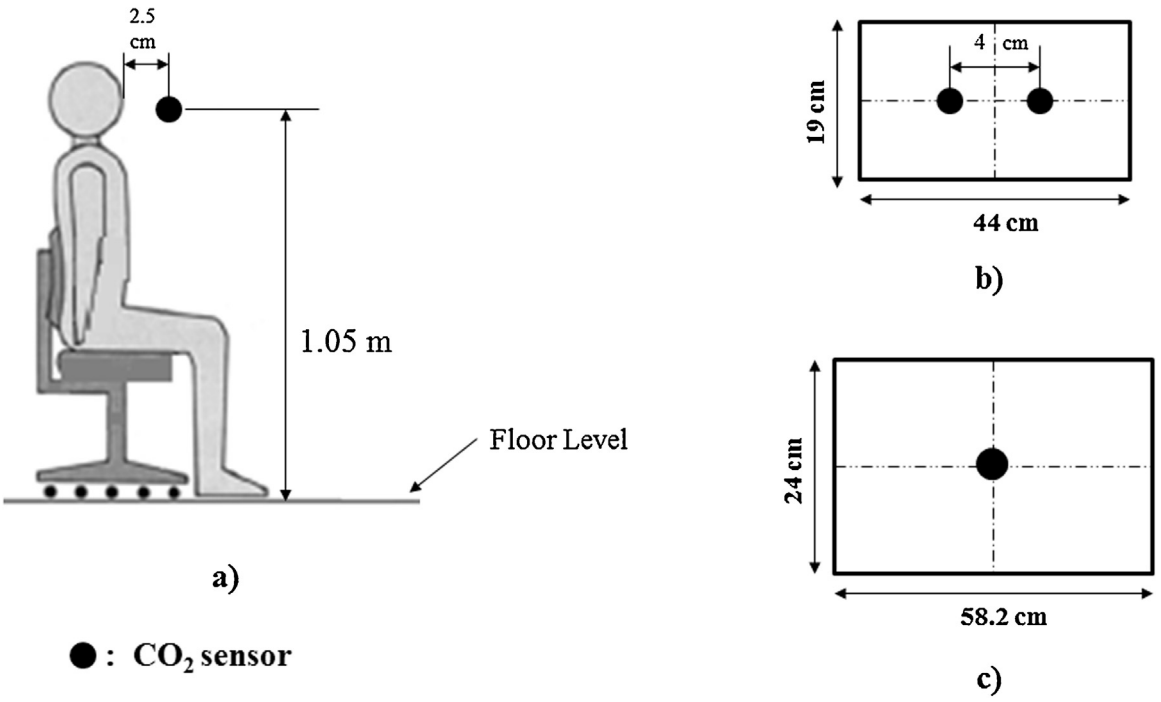

Fig. 6. Measurement locations of CO_2 concentration sensor (a) breathing zone of thermal manikin, (b) exhaust diffuser, and (c) supply diffuser.

age of 12 V and maximum power of 6.25 W. ABK precision 731A thermo anemometer was installed downstream of the fans. It is characterized by an accuracy of ±2% of full scale with a velocity measurement ranging between 0.1 m/s and 10 m/s. The airflow through each fan was adjusted by varying the supply voltage using a 12 V DC—Dimmer resulting in a flow rate ranging between 0 and 10 L/s/fan.

An internal load of 30 W/m^2 was generated in the room due to the presence of lighting and heat flux through the walls (no perfect insulated walls) resulting in 135 W, and thermal manikin generating 70 W.

For air quality assessment, a constant CO_2 dose of 2 L/min at room temperature was used representing the ambient passive contaminants. The CO_2 dose was equally distributed over four identical sources placed on each wall such that each source supplied 0.5 L/min of CO_2. Sampling tests for CO_2 were conducted by measuring the CO_2 concentration using FIGARO CDM4161-CO_2 sensors having an accuracy of ±20 ppm. The CO_2 sensors were connected to OMEGA DacPro data logger to store data and check stabilized residuals. Fig. 6(a)–(c) shows the measurement locations of the CO_2 concentration sensor. Accordingly, the CO_2 sensors were located at three different positions; two at the breathing level of thermal manikin where one sensor was located at a distance of 2.5 cm from the manikin's nose and the other was used as a backup sensor (no data was taken from the backup sensor so it is not shown in Fig. 6(a)); two at the middle section of the exhaust for accurate measurement where the average value was considered, and one at the middle section of the supply diffuser as it was measuring CO_2 concentration in the fresh air.

2.3. Experimental protocol

Prior to each set of measurements, the light was turned on; the thermal manikin was set to constant heat flux of 39 W/m^2 equally distributed over body segments. After attaining steady state conditions, the standalone DV system was turned on. The DV supply air flow rate and temperature were set to 80 L/s and 21.5 °C, respectively. The passive contaminant source located at a level of 1 m above the floor was introduced into the room. The CO_2 concentration in the supplied fresh air was checked to be within the fresh air CO_2 limit ranging between 300 ppm and 500 ppm. Since the experimental set up was held under steady state conditions, the CO_2 concentration and segmental surface temperature fields were monitored continuously until reaching stabilized values which occurs within an experimental period of 2 h.

The performance of the standalone DV system was compared to (DV + CF) system. The fans were set to two different heights of 25 cm and 40 cm above the floor while supplying a total flow rate of 25 L/s. The same procedure was repeated until the readings of the CO_2 and segmental surface temperature fields were stabilized. Each experiment was repeated three times to ensure precision and accuracy. A total of nine experiments were conducted including the repeated ones.

3. Results and discussion

3.1. CFD validation

The CFD validation is performed for the conditions of the experiment where the DV supply flow rate was and corresponded to an air change rate of 14.96 per hour for the room geometry. However, the characteristic of the DV system based on CFD simulations were still preserved through the presence of the generated thermal plumes from the heat sources and the observation of a stratification height that separates the space to two distinct lower clean zone and upper recirculation zone. The high velocity case is more critical for validation purposes because the physics of the DV flow and thermal plume interaction with room air might be altered by high supply velocity values. At lower supply flow rates, the deterioration of physical behavior associated with the DV system will not occur as long as the critical case of high velocity provided the characteristics of DV system. In addition, the airflow behavior around the thermal manikin in the presence of chair fans for low and high supply velocities were dominated by the higher velocity flow field induced by the fans.

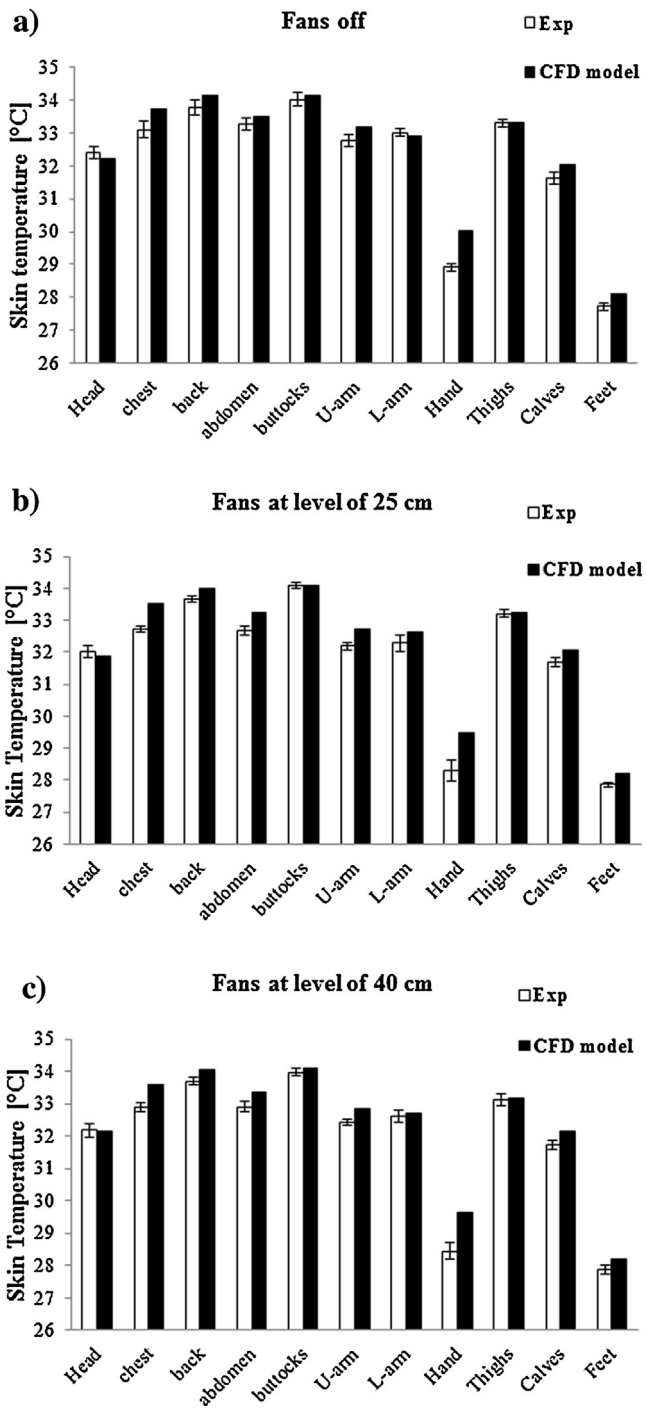

Fig. 7. Segmental surface temperature validation: (a) fans off (b) fans at level of 25 cm, (c) fans at level of 40 cm; total fans flow rate of 25 L/s.

Fig. 7 shows the predicted and experimental values of the segmental surface temperature for different fan configurations (a) fans off, (b) fans at level of 25 cm, and (c) fans at level of 40 cm. It is clear that the fans at the two heights reduced the segmental surface temperature mainly at the upper body parts (head, chest, abdomen, U-arm, L-arm, and hands). This is due to the improvement in the convective currents near the body segments. On the other hand, it is observed that the segmental surface temperature increased as the height of fans is increased. At 40 cm height compared to fans at a level of 25 cm, the surface temperature at the head and upper arm increased by 0.26 °C and 0.11 °C respectively. This could be justified by the principle of DV and fans operation. Due to buoyancy effects, the temperatures of air layers away from the floor level are hotter than those near the floor level. The fans placed at high level would draw air layers that are relatively warmer than those drawn by fans placed at low levels. This explains the increase in segmental surface temperature that was depicted as the position of fans was shifted from 25 cm to 40 cm above the floor. The results showed good agreement between predicted and measured segmental surface temperatures with a maximum relative error of 4.02% reported at the hands as shown in Fig. 7(a–c).

The air quality is assessed using the ventilation effectiveness (ε_v). Fig. 8 presents the predicted and experimental values of ventilation effectiveness for different fan configurations at 1 m source location. The results reveal that the fans at the two heights improved the ventilation effectiveness to reach a maximum of 38% when fans are set at a level of 25 cm. This is due to the ability of fans in drawing fresh air from lower levels and blowing it upwards towards occupant's breathing zone. On the other hand, an increase in fans height above the floor resulted in a drop in ventilation effectiveness i.e. (38% versus 34%). The relatively contaminated air drawn by the high level fans and delivered to the breathing zone at high momentum could justify this decrease in ventilation effectiveness. The results showed good agreement between experimental and measured values with a relative error ranging from 3.54% to 5.84%.

3.2. Parametric study

The validated CFD model results showed a clear dependence of segmental skin temperature and IAQ on the variation of height of fans above the floor for the two considered heights. Accordingly, finding the optimum height is of interest. To this aim, a typical office space is studied at inner dimensions 3.4 m × 3.4 m × 2.6 m with supply and return grills cross-sectional area of 3 m (width) × 0.1 m (height) and 0.5 m (width) × 0.2 m (height) respectively as shown in Fig. 2. The room air temperature is set to 25 °C. The passive contaminant source is assumed to produce 2 L/min of CO_2 at room temperature equally distributed over four identical sources located at each side wall where each source supplied 0.5 L/min of CO_2 to guarantee uniform distribution of contaminants within the room. The load in the room is set to 40 W/m^2 representing a typical maximum load removed by a DV system as reported by Yuan et al. [1] and Vivian et al. [25]. This load is generated as a result of typical lighting load of 10 W/m^2 [2]; desktop computer of 93 W [2]; an office occupant of 70 W under sedentary activity [2]; and the remaining load is assumed generated by the walls. The operating conditions are selected such that they provide a stratification height of 1.1 m which is the minimum stratification height recommended by ASHRAE standard [2] and are capable of removing the load generated in the room. Accordingly, the supplied fresh air is set to 21 °C and 47.5 L/s. The selection of the optimized height for the fans will be based on the assessment of three different parameters including total flow rate of fans $(\dot{Q})$, height of fans above the floor (H_{fs}), and passive contaminant height above the floor (H_s). Table 2 presents the simulated cases used in the parametric study. Furthermore, an energy analysis will be conducted to check the energy savings provided by the novel system when compared to a standalone DV system providing approximately same thermal comfort and IAQ levels.

3.2.1. Effect of height and flow rate of fans

3.2.1.1. Air quality. Fig. 9 shows a comparison between different configurations of fans on the basis of ventilation effectiveness. A standalone DV system (Fans off) resulted in a ventilation effectiveness of 49%. For fans at a level of 25 cm, as the flow rate increases, the ventilation effectiveness also increases to reach a maximum of 55% at 12 L/s and then decreases to 52% at 16 L/s. Unlike the case when

3.2.1.2. Thermal comfort.

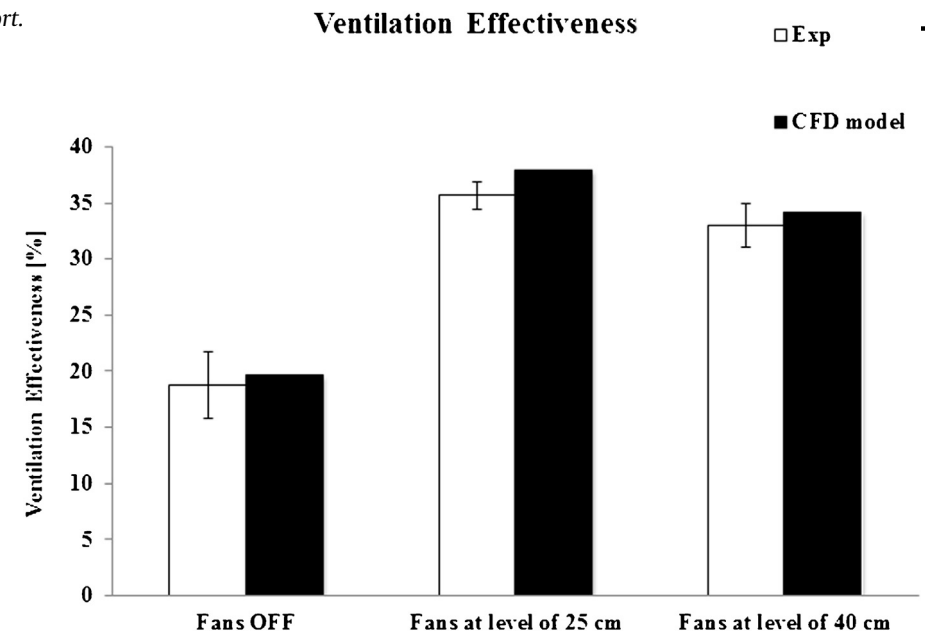

Fig. 8. The measured and predicted ventilation effectiveness for different fan configurations at 1 m source location.

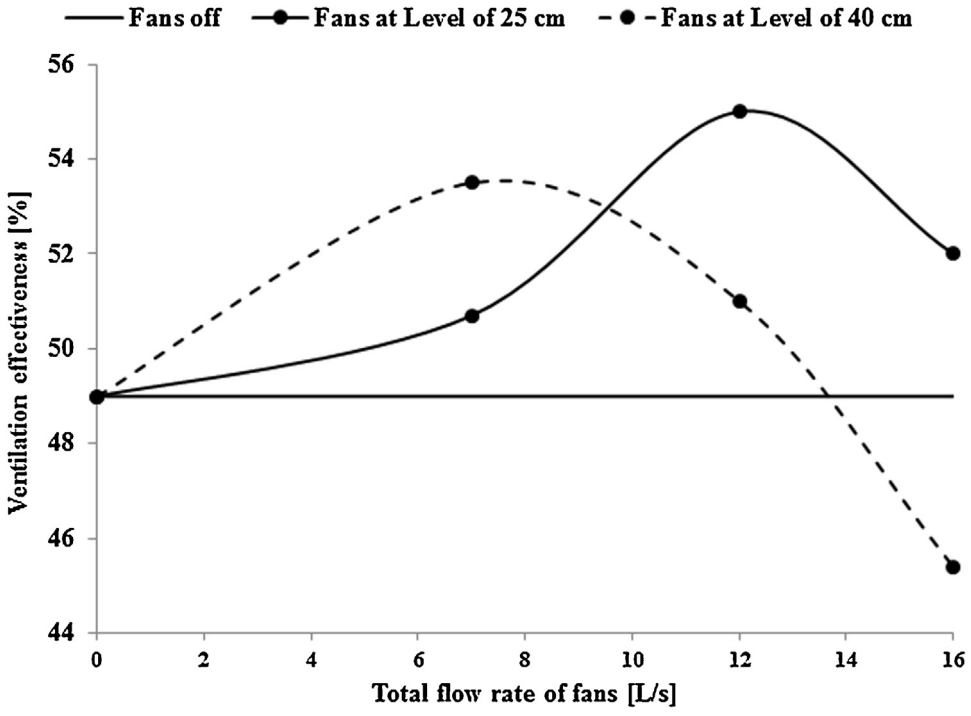

Fig. 9. Comparison of ventilation effectiveness at different fans levels and fans flow rates at 1 m source location.

fans are at a level of 40 cm, the ventilation effectiveness reached a value of 53.4% at low flow rate of 7 L/s which is higher than the value reached at a level of 25 cm for the same flow rate. This effectiveness is further reduced as flow rate increases to reach a value of 45.4% at 16 L/s indicating deteriorated IAQ compared to a standalone DV system.

The use of fans resulted in an increase in ventilation effectiveness since fans delivered fresh air from low levels towards the occupant's breathing zone. For low flow rate of fans, placing the fans at higher level increased the momentum of the drawn fresh air to reach the breathing zone resulting in good IAQ. On the other hand, placing the fans at low level while increasing their flow rate resulted in more fresh air delivered to the breathing zone at high momentum. However, excessive increase in flow rate would increase the tendency of mixing with more contaminated air resulting in decrease in ventilation effectiveness. For high level fans, the increase in flow rate of fans resulted in more contaminated air drawn from the middle zone, delivered to the breathing zone at high momentum, and mixed with more contaminated air resulting in low and degraded IAQ. Evidently, the use of fans improved ventilation effectiveness by 12.24% in the best scenario (fans at a level of 25 cm while supplying 12 L/s) and reduced effectiveness by 7.35% in the worst scenario (fans at a level of 40 cm while supplying 16 L/s).

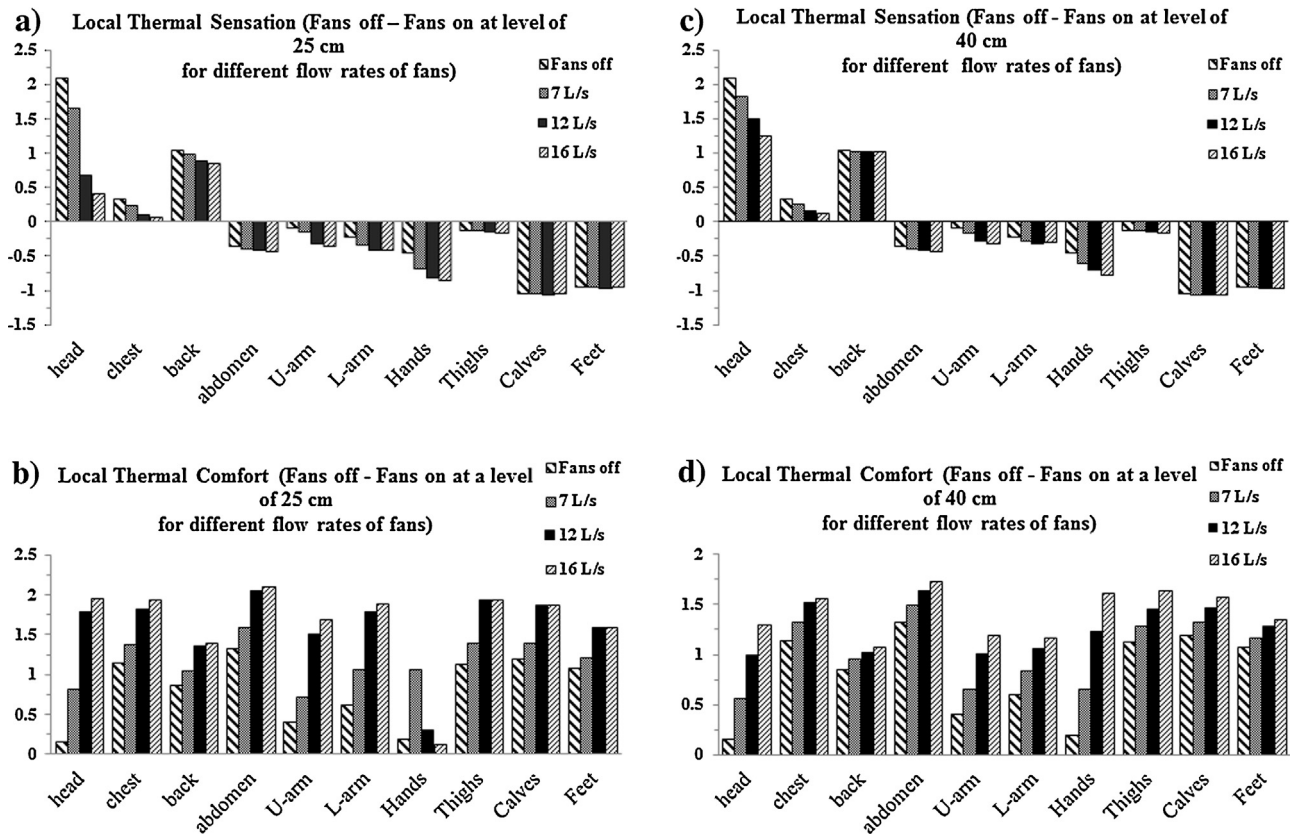

Fig. 10. Local thermal (a and c) sensation (LTS) and (b and d) comfort (LTC) for different fans configurations.

Table 2
Simulated cases used in parametric study.

Simulation Cases	Passive contaminant source height (m)	Height of fans (cm)	Total flow rate of fans (L/s)
Set 1	1	25	7
			12
			16
		40	7
			12
			16
Set 2	0.3	25	7
			12
			16
		40	7
			12
			16

Fig. 10 illustrates (a) local thermal sensation (LTS) and (b) local thermal comfort (LTC) for Fans off – Fans on at level of 25 cm for different flow rate of fans and (c) LTS and (d) LTC for Fans off – Fans on at level of 40 cm for different flow rate of fans. Fig. 11 presents the velocity contours for (a) Fans off, (b), Fans on at a level of 25 cm, and (c) Fans on at a level of 40 cm while supplying a total flow rate of 12 L/s. Compared to a standalone DV system (Fans off), the upper body parts (head, chest, abdomen, U-arm, L-arm, and hands) are the segments mostly affected by fans operation. This is clearly illustrated by the drop in LTS accompanied by an increase in LTC as shown in Fig. 10(a)–(d) and clearly presented by the velocity contours over the upper body parts as shown in Fig. 11(a)–(c). However, the use of fans at different heights and flow rates resulted in variation in occupant thermal response.

Table 3 presents the overall thermal sensation (TS) and overall thermal comfort (TC) for different fan configurations that are simulated. For the case when fans are off, the TC of an office occupant reached 0.8. For the case of 25 cm, as the flow rate is increased, TC increases to reach a maximum of 1.24 at 12 L/s and then decreases to reach a value of 1.18 at 16 L/s. However, for the case of 40 cm, as the flow rate is increased, the TC continues increasing to reach a value of 1.4 at 16 L/s. In both locations of fans, the increase in TC attributed to the enhancement of the convective currents near the occupant as shown in Fig. 11(a)–(c). Compared to a standalone DV system, at low flow rate of 7 L/s, the enhancement in TC is at a lower rate when fans are shifted from a level of 25 cm to 40 cm. This could be justified by the ability of low-level fans to draw cooler air at favorable thermal sensation (0.59 versus 0.68). Conversely, an improvement in TC is observed at high flow rates as the fans are shifted from 25 cm to 40 cm (see Table 3). As shown in Fig. 11(b) and (c), the variation in the convective currents near the upper body segments for the same fans flow rate at different fans height could be related to the temperature difference resulting between the occupant surface temperature and environment. For fans supplying 12 L/s, and placed at a level of 25 cm and 40 cm above the floor, the thermal sensation reported a value of 0.17 and 0.53 respectively (see Table 3) indicating lower segmental surface temperature when fans were at a level of 25 cm; thus, strengthening the thermal plume (higher temperature difference results in higher velocity). Accordingly, the low values of TC reported for low-level fans could be attributed to fans drawing cooler air and blowing it at high velocity resulting in thermal draft sensation. However, the increase in fans velocity overcame the hot air layers drawn by high level fans providing comfortable thermal conditions. Evidently, compared to a standalone DV system, the fans provided the occupant with comfortable environment resulting in low improvement in TC of 35% (fans at a level of 40 cm while supplying 7 L/s) and high improvement in TC of 75% (fans at a level of 40 cm while supplying 16 L/s).

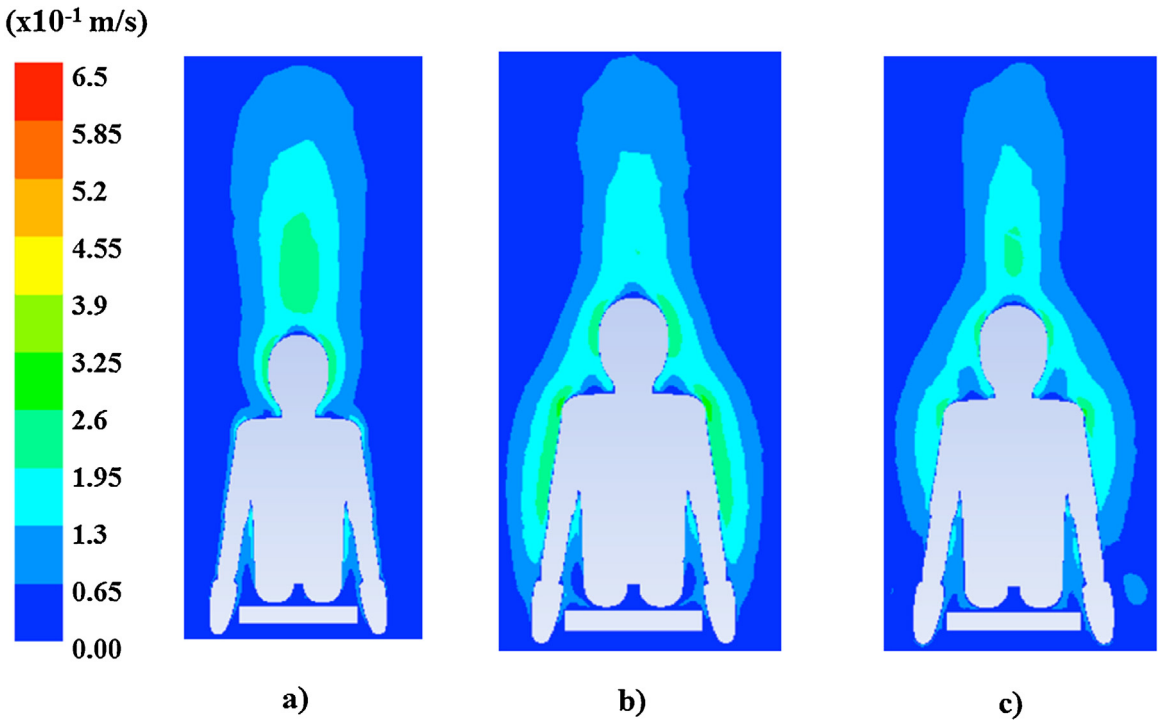

Fig. 11. Velocity contours for different fans configuration (a) fans off, (b) fans at a level of 25 cm, and (c) fans at a level of 40 cm for the case of 12 L/s total fans flow rate.

Table 3
The overall thermal sensation (TS) and overall thermal comfort (TC) for different fan configurations.

Fans off		Total flow rate of fans (L/s)	Fans at level of 25 cm		Fans at level of 40 cm	
TS	TC		TS	TC	TS	TC
0.82	0.8	7	0.59	1.19	0.68	1.08
		12	0.17	1.24	0.53	1.32
		16	0.14	1.18	0.43	1.4

Sun et al. [5] reported that the optimal fan speed ranged between 0.48 m/s and 1.22 m/s with the percentage of people dissatisfied reaching a value of 26% when fans placed near the thighs at 24 °C room temperature and 30 L/s supply flow rate. The findings of the current study for the same room geometry and location of fans of Sun et al. [5] were shown to result in an optimal fan speed of 0.625 m/s which is with the range predicted by Sun et al. [5] while providing acceptable thermal comfort levels of 1.4 based on Zhang's model [21–23] for a room at 25 °C and 47.5 L/s supply flow rate. Although, the TC level was determined using a different comfort model from that used by Sun et al. [5], both models resulted in acceptable comfort levels.

In presence of passive contaminant source, Sun et al. [7,8] reported that the use of fans increase contaminant concentration near the breathing zone of the thermal manikin when fans were supplying 11.9 L/s and placed near the thighs. The current study showed that the fans could improve or deteriorate the performance of the (DV + CF) based on selected fans flow rate and height above the floor. However, for the similar location of fans above the floor used by Sun et al. [7,8], the current study shows negative effect of fans while supplying a flow rate of 16 L/s. Hence, the results indicated that it is possible for the fans to increase contaminant concentration even though simulation showed a higher fan flow rate which could be related to different reasons related to diffuser supply flow rate, room dimensions, etc. The risk of cross contamination when the human body is a polluting source was studied by Sun et al. [5,7,8] where the contaminant transportation between two thermal manikins (polluted and exposed manikins) increased when only one of the thermal manikins used chair fans and the other did not. In a different study, Habchi et al. [11] reported that particle transmissions between two thermal manikins (infected and exposed manikins) decreased when both thermal manikins used chair fans.

3.2.1.3. Height optimization. As stated in the previous sections, the interrelation between height and flow rate of fans affected the performance of the novel system. Similar to the study done by Sun et al. [7], the fans were placed symmetrically with respect to the occupant representing general occupant posture. Therefore, an optimum height that could provide the best combination of TC and IAQ was highly recommended. Accordingly, the two different indices (TC and ventilation effectiveness) are plotted for three different flow rates where the compromised height is selected based on the intersection between the two indices. Fig. 12 shows the criterion for height selection when fans are supplying 16 L/s. Table 4 illustrates the selected heights and their corresponding TC, enhancements in TC, ventilation effectiveness, and enhancements in ventilation effectiveness when compared to the case when fans are Off.

To check the energy savings of the proposed novel system, the energy consumed consumption by (DV + CF) system is compared to a standalone DV system providing approximately the same TC and air quality. Accordingly, a chiller with an average COP of 3.5 is selected. Fresh air at 32 °C and 70% RH supplied by a fan is cooled and dehumidified by exchanging heat with a cooling coil provided by the chiller where it is extracted from the room by an exhaust

Table 4
The selected heights and their corresponding TC, enhancements in TC, ventilation effectiveness and enhancements in ventilation effectiveness along with the energy savings for three different fans flow rate (7 L/s, 12 L/s, and 16 L/s) for a source at a level of 1 m above the floor.

Cases with source at 1 m Total flow rate of fans (L/s)	Optimum height of fans (cm)	TC	Enhancement in TC (%)	ε_v (%)	Enhancement in ε_v (%)	Energy savings (%)
7	30.2	1.148	43.5	52.4	6.94	9.3
12	30.9	1.407	75.9	54.4	10.9	20.6
16	32.7	1.332	66.5	50	2.1	1.1

Table 5
The selected heights and their corresponding TC, enhancements in TC, ventilation effectiveness, and enhancements in ventilation effectiveness along with the energy savings for three different fans flow rate (7 L/s, 12 L/s, and 16 L/s) for a source at a level of 0.3 m above the floor.

Cases with source at 0.3 m Total flow rate of fans (L/s)	Optimum height of fans (cm)	TC	Enhancement in TC (%)	ε_v (%)	Enhancement in ε_v (%)	Energy savings (%)
7	26.5	1.178	47.3	25.25	26.9	6.5
12	30.1	1.39	74	28.3	42.2	11.6
16	31.2	1.309	63.6	27.9	40.2	10.2

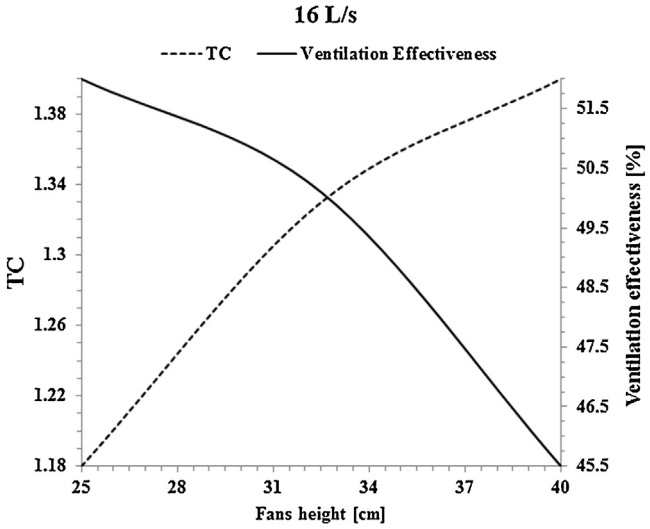

Fig. 12. Selected height for fans supplying 16 L/s.

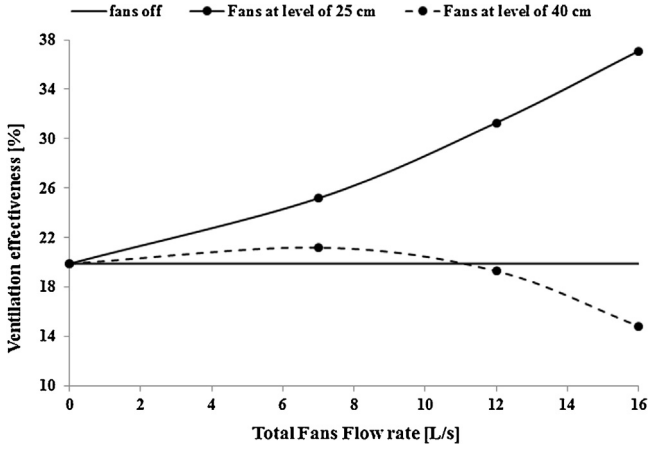

Fig. 13. Comparison of ventilation effectiveness at different fans levels and fans flow rates at 0.3 m source location.

fan. The electrical power consumed by the chiller would be added to the electrical power consumed by the fans. The chair-mounted fans consumed a power of 25 W. The energy savings for the selected heights was evaluated and tabulated as shown in Table 4. Accordingly, for the current thermal environment, it is recommended to place the fans at 30.9 cm while supplying 12 L/s and providing 20.6% energy savings.

3.2.2. Effect of source height

The purpose of this study is to check the effect of fans when the passive contaminant source height is varied. For the current study, fan configurations along with the DV supply flow rate and temperature are held similar to those used in the previous sections; however, the passive contaminant source is shifted to a level of 0.3 m above the floor. As expected, changing the source height would only affect the air quality in the room. Fig. 13 presents a comparison based on ventilation effectiveness between different fan configurations for a source located at 0.3 m.

Comparing Figs. 9 and 13; for the case of fans off, the ventilation effectiveness decreases to reach a value of 19.9%, when the source level is shifted from 1 m to 0.3 m above the floor. The layer near the floor level became highly contaminated when the source is located at 0.3 m, which in turn delivered higher contaminated air to the breathing zone resulting in degraded IAQ. On the other hand, for a source located at 0.3 m, when fans are positioned at 40 cm above the floor and their flow rate is increased, the ventilation effectiveness follows the same trend depicted when the source is located at 1 m. For fans at a level of 25 cm and, unlike the case of 1 m source, as the fans flow rate is increased, the ventilation effectiveness continues increasing to reach a value of 37.1% at 16 L/s. The observed difference is due to the different interactions between the drawn air by fans and the contaminants produced by the passive source.

Following the same procedure used in Section 3.2.1.3, the selected heights and their energy savings for different flow rates of fans at a source level of 0.3 m is illustrated in Table 5. Accordingly, for the current thermal environment, it is recommended to place the fans at a level of 30.1 cm while supplying 12 L/s and providing 11.6% energy savings.

4. Conclusion

A validated CFD model is integrated with a validated bio-heat model to select the optimized height of fans above the floor that can provide acceptable TC and good IAQ at the least energy consumption. This assessment is based on varying fans flow rate, fans height above floor, and contaminant source height above floor. The interrelation between these parameters and their effect on TC and IAQ led to optimal fans heights of 30 cm and 31 cm above the floor for a pollutant source located at 1 m and 0.3 m above the floor respectively, while fans were supplying a total flow rate of 12 L/s. Moreover, the assessment revealed that, for an optimal height of fans above the floor, an energy savings of 11.6% and 20.6% was reported when the novel system was compared to a standalone DV system.

References

[1] X. Yuan, Q. Chen, L.R. Glicksman, A critical review of displacement ventilation, ASHRAE Trans. 104 (1A) (1998) 78–90.
[2] ASHRAE Handbook—Fundamentals, American Society of Heating Refrigerating and Air-Conditioning Engineers, Atlanta, 2009, Chapter 9.
[3] H. Skistad, E. Mundt, P.V. Nielsen, V. Hagström, J. Railio, Displacement ventilation in non-industrial premises, in: REHVA Guidebook No. 1, Federation of European Heating and Air-conditioning Associations—REHVA, Brussels, 2002.
[4] H. Brohus, P.V. Nielsen, Personal exposure in displacement ventilated rooms, Indoor Air 6 (3) (1996) 157–167.
[5] W. Sun, D. Cheong, A. Melikov, Subjective assessment of thermal environment in a room ventilated by a novel enhanced displacement ventilation system, in: Proceedings of the 11th International conference on Indoor Air Quality and Climate—Indoor Air, 17–22 August 2008, Copenhagen Paper ID: 963, 2008.
[6] W. Sun, K.W.D. Cheong, A.K. Melikov, Subjective study of thermal acceptability of novel enhanced displacement ventilation system and implication of occupants' personal control, Build. Environ. 57 (2012) 49–57.
[7] W. Sun, Study of enhanced displacement ventilation in office environment in the tropics, in: Doctoral Dissertation, National University of Singapore, 2010.
[8] A. Sun, Distribution of contaminants in the occupied zone of a room served by a novel enhanced displacement ventilation system, in: Proceedings of AIVC 2008 Conference, Kyoto, Japan, 14–16 October, 2008.
[9] W. Sun, D. Cheong, A. Melikov, Impact of different types of fans in a novel enhanced displacement ventilation system on vertical temperature profile and air distribution in a field environment chamber, in: Proceedings of The First International Conference on Building Energy and Environment, (COBEE, 2008), July 13–16, Dalian, China, paper, 2008.
[10] A. Sun, Local climate and heat loss from human body with a novel enhanced displacement ventilation system, in: Proceedings of the 11th International conference on Indoor Air Quality and Climate—Indoor Air, 17–22 August 2008, Copenhagen, Paper ID: 962, 2008.
[11] C. Habchi, K. Ghali, N. Ghaddar, A. Shihadeh, Chair fan-enhanced displacement ventilation for high IAQ: effects on particle inhalation and stratification height, Build. Environ. 84 (2015) 68–79.
[12] B. El-Fil, N. Ghaddar, K. Ghali, Optimizing performance of ceiling-mounted personalized ventilation system assisted by chair fans: assessment of thermal comfort and indoor air quality, Sci. Technol. Built Environ. 22 (4) (2016) 412–430.
[13] A. Makhoul, K. Ghali, N. Ghaddar, Desk fans for the control of the convection flow around occupants using ceiling mounted personalized ventilation, Build. Environ. 59 (2013) 336–348.
[14] A. Makhoul, K. Ghali, N. Ghaddar, Low-mixing coaxial nozzle for effective personalized ventilation, Indoor Built Environ. 22 (3) (2013) 508–519.
[15] ANSYS Software ANSYS Inc., Southpoint, Canonsburg, PA 15317, USA http://www.ansys.com/.
[16] P. Zelenský, M. Barták, J.L.M. Hensen, R. Vavřička, Influence of turbulence model on thermal plume in indoor air flow simulation, Proceedings of the 11th REHVA World Congress "Energy Efficient, Smart and Healthy Buildings" (Clima) (2013).
[17] M.P. Wan, C.Y. Chao, Numerical and experimental study of velocity and temperature characteristics in a ventilated enclosure with under floor ventilation systems, Indoor Air 15 (5) (2005) 342–355.
[18] M. Kanaan, N. Ghaddar, K. Ghali, G. Araj, New airborne pathogen transport model for upper-room UVGI spaces conditioned by chilled ceiling and mixed displacement ventilation: enhancing air quality and energy performance, Energy Convers. Manage. 85 (2014) 50–61.
[19] ANSI/ASHRAE, Ventilation for acceptable indoor air quality, in: ANSI/ASHRAE. Standard 62. 1-2013, American Society of Heating, Air- Conditioning and Refrigeration Engineers Inc., Atlanta, 2013.
[20] M. Salloum, N. Ghaddar, K. Ghali, A new transient bioheat model of the human body and its integration to clothing models, Int. J. Therm. Sci. 46 (4) (2007) 371–384.
[21] H. Zhang, E. Arens, C. Huizenga, T. Han, Thermal sensation and comfort models for non-uniform and transient environments, part I: local sensation of individual body parts, Build. Environ. 45 (2) (2010) 380–388.
[22] H. Zhang, E. Arens, C. Huizenga, T. Han, Thermal sensation and comfort models for non-uniform and transient environments, part II: local comfort of individual body parts, Build. Environ. 45 (2) (2010) 389–398.
[23] H. Zhang, E. Arens, C. Huizenga, T. Han, Thermal sensation and comfort models for non-uniform and transient environments, part III: Whole-body sensation and comfort, Build. Environ. 45 (2) (2010) 399–410.
[24] Epoxy Thermal Manikin, Instruments For Textile & Biophysical Testing. Seattle, WA, [Online], Available: http://www.thermetrics.com/sites/default/files/product_brochures/NEWTON%20Manikin_Spec%20Sheet.pdf.
[25] L. Vivian, B. Rohini, M. Michelle, V. Edward, M. Mike, Energy Savings Potential of Flexible and Adaptive HVAC Distribution Systems for Office Buildings, ARTI21-CR Research Project (2002) 605-30030.